ON THE FUEL CYCLE AND NEUTRON FLUXES OF THE HIGH FLUX REACTOR AT ILL GRENOBLE*

D. Ridikas†, G. Fioni, P. Goberis, O. Déruelle, M. Fadil, F. Marie, S. Röttger

DSM/DAPNIA/SPhN, CEA Saclay, F-91191 Gif-sur-Yvette Cedex, France

Abstract

The fuel evolution and neutron fluxes of the High Flux Reactor at ILL Grenoble were investigated for the full fuel cycle. Two different code systems, namely *Monteburns* and MCNP+CINDER'90, were employed for a realistic 3D-geometry description of the reactor core and experimental channels of interest. Both codes reproduce correctly the history of the fuel burnup. Calculated neutron flux in the reactor core is $2.16\times10^{15}\frac{n}{s\,cm^2}$ and decreases down to $1.65\times10^{15}\frac{n}{s\,cm^2}$ and $6.7\times10^{14}\frac{n}{s\,cm^2}$ in the experimental channels V4 and H9 respectively. Thermal neutron contribution is ~85.2% in V4 and ~98.3% in H9. We show that neutron fluxes in the experimental channels V4 and H9 are not perturbed/changed due to the burnup of the fuel element and/or move of the control rod. This result should simplify most of the irradiation experiments (and data analysis in particular), which employ the experimental channels as above.

*To be published in the Proceedings of the 5th Int. Specialists' Meeting SATIF-5, OECD/NEA Paris (2000).

†E-mail: ridikas@cea.fr

Introduction

In the frame of the Mini-Inca project [1] – integral measurements relevant to nucler waste transmutation systems – neutron beams delivered by the High Flux Reactor of the Institut Laue-Langevin in Grenoble [2] will be used, both for thermal and epithermal spectra. The choice of the ILL reactor for nuclear waste transmutation related projects is mainly due to its unique possibility to dispose of several different neutron spectra, obtained by changing the distance between the sample and the fuel element (core). It also provides very high thermal neutron flux ($\sim 10^{15} \frac{n}{s\,cm^2}$), which makes possible high accuracy measurements in the thermal energy region with a very small amount of target material ($\sim 10 \mu$g) [1].

So far, there was no quantitative and consistent study of neutron fluxes delivered by the ILL reactor to the experimental channels. In principle, these fluxes may change due to the nuclear fuel burnup and/or move of the control rod during the full reactor cycle of ~50days. There is no doubt that variable irradiation conditions could influence/complicate data analysis if neutron fluxes are considerably changed as a function of time.

Here we perform quantitative calculations of the fuel evolution and corresponding comparison (time-dependence) of the neutron fluxes both in the reactor and experimental channels. A realistic 3-D geometry of the reactor core and experimental tubes of interest is modelled with two different code systems, namely *Monteburns* and MCNP+CINDER'90.

Simulation codes and data libraries

Below we briefly describe the code systems employed to perform the fuel evolution and neutron flux calculations. By comparing the results obtained with two different codes we want to make sure that our simulations are reliable and self consistent.

An automatic Monteburns code

Monteburns [3] was designed to link the Monte Carlo N-Particle Transport Code MCNP [4] and the radioactive decay and burnup code ORIGEN2 [5] into an automated tool. MCNP generates a statistical history for a neutron based random samples from probability distributions. These distributions are used in calculations to determine the type of interaction the particle undergoes at each moment of its life, the resulting energy of the particle if it scatters, if it is absorbed, the number of particles that "leak" from the system because of geometry constraints, and the number of neutrons produced if the neutron causes a fission or (n,xn) reaction. The fluxes of neutrons determined in this way can then be used to tally a wide variety of information (reaction rates, heating rates, doses, etc.) for the system.

The main function of the *Monteburns* is to transfer one-group cross section and flux values from MCNP to ORIGEN2, and then transfer the resulting material compositions (after irradiation and/or decay) from ORIGEN2 back to MCNP in a repeated, cyclic fashion. ORIGEN2 performs burnup calculations for *Monteburns* using the matrix exponential method in terms of time-dependent formulation, destruction and decay concurrently. The nuclides contained in the ORIGEN2 data bases have been divided into three segments: 130 actinides, 850 fission products, and 720 activation products (a total of 1700 nuclides) [5].

Monteburns produces a large number of criticality and burnup results based on various material feed/removal specifications, given power, and time intervals. The results obtained from

Monteburns are more accurate if long irradiation periods are broken up into several intervals of time because the physics and composition of materials in the system may change significantly with time. Not all isotopes produced during the burnup step are transfered for a follow-up MCNP calculation. If an isotope contributes a large enough fraction to absorption or fission interactions, mass or atom density, then automatically the isotope is considered "important". Flux and one-group, spectrum-averaged, cross-section tallies can then be performed in MCNP for these isotopes (except those for which no MCNP cross section exist).

Monteburns calculations are only as good as the MCNP cross-sections that are available to the user (e.g., see Refs. [6, 7, 8]). *Monteburns* is also limited by the accuracy of the ORIGEN2 fission product yields and decay data library.

Manual coupling of MCNP and CINDER'90 codes

Instead of using *Monteburns*, an interesting alternative is to run CINDER'90 transmutation inventory code [9] coupled to MCNP because of increased output options, improved default cross-section sets (for 63-group neutron energies) and fission product yields, and possibly wider availability (e.g. handling of the spallation products in high-energy induced reactions). However, coupling of CINDER'90 to MCNP is not yet available in the automatic-cyclic fashion. Therefore, averaged 63-group neutron fluxes have to be recalculated with MCNP for each consequent burnup step, for which MCNP materials are feeded manually as a result of the previous CINDER'90 burnup output.

In brief, the temporal concentrations of nuclides depleted and produced in materials subject to irradiation are described by a large set of coupled differential equations, each nuclide's concentration being determined by a history of gains from neutron absorption reactions (spallation, fission, (n,γ), (n,2n), etc.) and radioactive decay of parent nuclides, and losses from its own decay and particle absorption. The CINDER'90 code resolves nuclide couplings into linear chains, resulting in small independent sets of differential equations describing the rate of change of partial concentrations of nuclides in each chain. The solution of a large sets of differential equations is thus reduced to the solution of a number of small sets of differential equations. Because of the linear nature of the chain (a result of Markov like process), the generalized equations are solved sequentially for the partial concentration of each linear nuclide in the chain. Nuclide concentrations are then obtained by summing partial concentrations (see [9] for more detailed description).

The CINDER'90 code has a library of 63-group cross sections (to be compared with one-group cross sections used by ORIGEN2). The library, known as *LibB*, of nuclear data used by CINDER'90, constantly growing in breadth and quality, now describes 3400 nuclides in the range $1 \leq Z \leq 103$ including 1325 fission products. CINDER'90 uses these data, e.g. ENDF/B-VI, Joint European Data File (JEF-1), European Activation File (EAF-3), Master Decay Library (MDL), GNASH code results, etc. [9].

The High Flux Reactor at ILL Grenoble

ILL reactor chracteristics

The high flux reactor of the Institute Laue-Langevin (ILL) in Grenoble provides the highest thermal neutron flux in the world for research purposes. A single fuel element of highly enriched uranium (93%) is cooled and moderated by a flow of heavy water. The main reactor characteristics employed in our simulations are given in Table 1. More details can be found in the

Reactor thermal output	$58\mathrm{MW}_{th}$
Average reactor cycle	$\sim$50days
Average core power density, (W/cm^3)	1253
Core geometrical parameters:	
- core radius, inner/outer (cm)	14.0/19.5
- core height (cm)	80.0
- inner radius of reflector (cm)	11.9
- axial reflector thickness (cm)	105.5
Control rod material	natural Ni
Initial fuel isotopic composition, (%)	
- U-235	93
- U-238	7
Core fuel inventory (g)	$\sim$ 8600
B-10 zone inventory (g)	$\sim$ 7.8

Table 1: Main characteristics of the high flux reactor at ILL Grenoble with higly enriched uranium fuel in equilibrium.

Ref. [2].

In Fig. 1 we present the major elements of the reactor geometry used for neutron flux estimations with the MCNP code. MCNP is run in the mode of the criticality eigenvalue (k_{eff}) problem.

The control rod changes its position (moves down) as a function of time (as a function of the evolution of the fuel composition) in order to keep k_{eff} $\sim$1. A position of the control rod at any time t is known experimentally for 50 days of the reactor fuel cycle [2]. We have followed this dependence during our simulations by changing MCNP input file. One has to note that the antireactivity of the control rod changes due to the irradiation from one cycle to another cycle. Therefore, depending on how many times (cycles) the same control rod was used, its position dependence might change. As a matter of fact, the control rod is replaced by a new one once per year.

Our calculations show that the worth of the control rod is $\sim$16500pcm. Another $\sim$5500pcm is due to upper and lower borated zones of the reactor (see Fig. 1). These values are in a good agreement with the ones reported in [2], i.e. 17300pcm and 4500pcm correspondingly.

A formulation of the problem

As we have already mentioned, the main goal of this study is to estimate the change (if any) of the neutron fluxes both in absolute value and energy due to the fuel evolution and/or move of the control rod of the reactor. Of course, the "theoretical" reactor should stay in equilibrium (k_{eff}=1) or as close to the equilibrated system as possible during its full fuel cycle we want to simulate. Another interest is related to the validation/comparison of two different evolution codes, namely ORIGEN2 and CINDER'90.

We use both *Monteburns* and MCNP+CINDER'90 code systems for the material evolutions of the fuel (core) and 2 borated zones as shown in Fig. 1. Reactor power is kept constant at $58\mathrm{MW}_{th}$ by means of an automatic renormalization (if needed) of the neutron flux. The absolute value of the neutron flux is calculated using the following expression [3]:

$$\phi = \phi_n \times C = \phi_n \times \frac{\nu\, P\, (10^6\, W/MW)}{(1.602 \times 10^{-13}\, J/MeV)\, k_{eff}\, Q_{ave}}, \qquad (1)$$

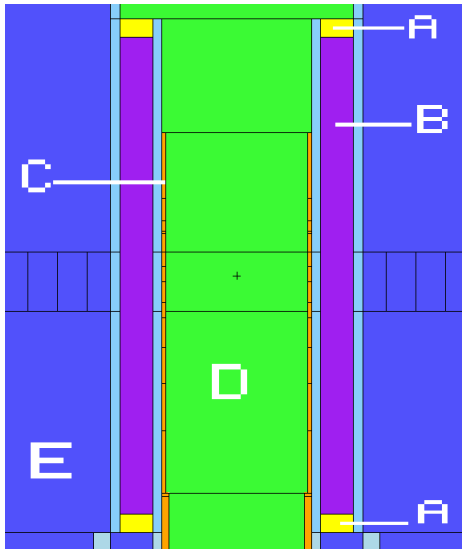

Figure 1: A representation of the major elements of the reactor geometry. The following notation is employed: A - borated zones, B - reactor core, C - control rod, D - inner reflector region, E - outer reflector region. Note: all elements have cylindric geometry and are symmetric along the central reactor axis.

where ν is an average number of neutrons produced per fission, P is a reactor power (in MW) defined by user, k_{eff} is an effective neutron multiplication factor given by MCNP and Q_{ave} is an average recoverable energy per fission, while ϕ_n stands for an average neutron flux obtained from the MCNP output file and normalized per source neutron.

50 days fuel cycle is then divided into 13 smaller intervals for which k_{eff} and fluxes in the reactor areas of interest are recalculated with new/updated material compositions (if these are considered "important" according to the conditions we have discussed in the previous Section).

Simulation results

Fuel burnup and k_{eff} of the reactor

The history of the fuel burnup is presented in Tables 3-4. In addition to the evolution of U-235, U-238 and Pu-239 we also represent the evolution of Xe-135 and Sm-149 (here as fission products and major neutron poisons) in the fuel element. The calculated burnup of U-235 is nearly 47.5% with *Monteburns* and 46.6% with MCNP+CINDER'90. These numbers are in a reasonable agreement with burnup rates given in Ref. [2], namely 36% on average and a possible maximum burnup of 70% during the full reactor cycle.

Table 3 also gives the calculated average flux intensities both in the fuel element (core) and in the experimental tubes V4 and H9 at their lowest/end positions (to be discussed in the following Section).

Fig. 2 represents the evolution of k_{eff} during the full reactor cycle. In order to keep the k_{eff} constant, the move of the control rod should compensate the fuel burnup (see Table 3), what is consistently reproduced by both simulations. This also proves that the evolution of the fuel and borated zones is done correctly.

The only big difference (between two codes) in the material composition of the fuel is seen

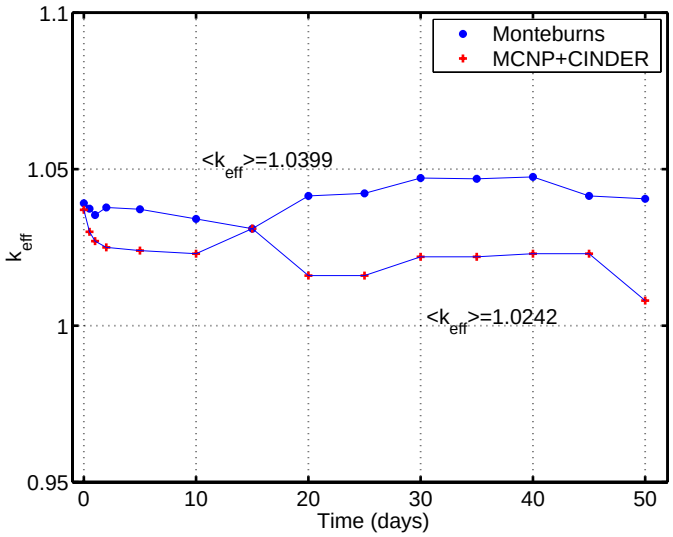

Figure 2: A variation of k_{eff} as a function of time during fuel cycle.

from the evolution of Pu-239 (compare the corresponding columns in Tables 3-4). The total mass of Pu-239 predicted by *Monteburns* is 3 times higher than the same quantity obtained with CINDER'90. Although this disagreement has no/little influence on the fuel cycle of the ILL reactor due to very small mass of Pu-239 produced, below we give a brief explanation.

In general, the processing of continuous-energy data into multigroup data is accomplished with a weighting flux, and that flux should be applicable to the problem. That is a huge requirement for a multigroup library that is used for thermal reactor problems and for accelerator transmutation. In Fig. 3 we compare 63-group neutron cross sections weighted with ILL core

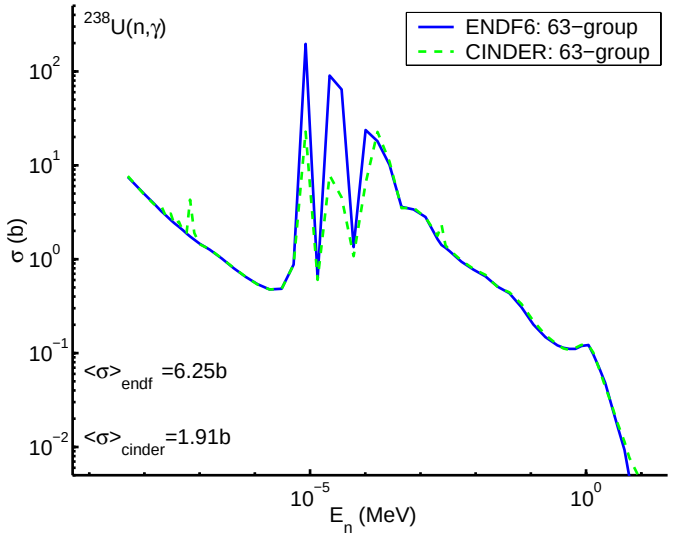

Figure 3: 63-group neutron cross sections of ^{238}U(n,γ) as extracted from CINDER'90 data library (dashed line) and processed from continuous-energy data by weighting with the ILL core flux (solid line).

flux (solid line) as calculated in this work and 63-group neutron cross sections extracted from CINDER'90 data library (dashed line), which was preprocessed by weighting with the PRS

(Power Reactor Studies) flux [9]. As one can see, both evaluations agree for low and fast neutrons, while they differ in the resonance region. In problems having a large resonance-region flux, such as thermal- and fast-reactors, the very abundant U-238 results in very great flux depressions at the energies of the U-238 resonances. The same factor of 3 we found in the difference of Pu-239 production now is present in an effective averaged (flux weighted) one-group ^{238}U(n,γ) cross section (see the same Fig. 3). The conclusion is that the prediction of Pu-239 mass given by *Monteburns* should be more accurate because a problem specific flux was employed in getting a corresponding effective one-group cross section, which was actually used in the evolution of fuel materials.

Neutron fluxes in the core

The main goal of this study was to estimate possible changes of the neutron fluxes due to the move of the control rod and fuel burnup. The time-dependent energy distributions of the neutron flux are presented in Fig. 4. These curves stand for the average neutron flux in the fuel

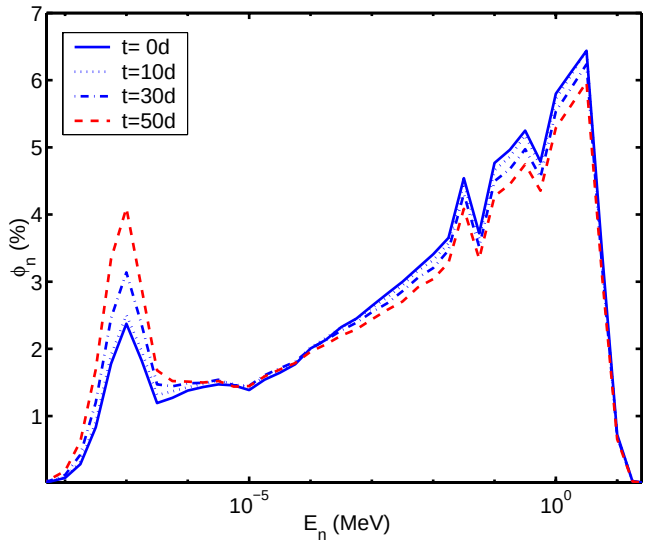

Figure 4: A variation of the average neutron spectrum inside the fuel element (core) during the reactor cycle of 50 days. The spectra presented are at time t=0, 10, 30 and 50 days.

element (core). It is clearly seen that there are more (by $\sim$7%) thermal neutrons (E_n <1eV) at the end of the fuel cycle, while the relative weight of the energetic neutrons has decreased correspondingly. The corresponding numbers are given in Table 2 explicitly.

The "thermalization" of the neutron flux in the core is mainly due to the move of the control rod; in this way more thermal neutrons can be rescattered back to the fuel element from the inner reflector region (D_2O). We remind here that the control rod moves down and at the end of the fuel cycle is completely withdrawn from the active zone (see Fig. 1 for a geometry of the core). In addition, the decrease/saturation of Xe-135 ($T_{1/2}$=9.1h) and Sm-149 concentrations (being the major poisons of thermal neutrons) also will have non negligible effect on the neutron energy spectra. The corresponding concentrations of Xe and Sm are given in Tables 3-4 for the

time, days	ϕ_n, % [0.,.1]eV	ϕ_n, % [.1,1.]eV	ϕ_n, % [1.,100.]eV	ϕ_n, % [.1,100.]keV	ϕ_n, % [.1,1.]MeV	ϕ_n, % [1.,20.]MeV
0.0	5.3	5.7	12.9	38.5	20.8	16.8
10.0	5.8	6.1	13.0	38.0	20.5	16.6
20.0	6.4	6.4	13.1	37.6	20.2	16.3
30.0	7.4	6.7	13.1	36.9	19.7	16.2
40.0	8.6	7.2	13.0	36.1	19.3	15.8
50.0	10.0	7.6	12.9	35.1	18.8	15.6

Table 2: A variation of the average neutron spectrum inside the fuel element (core) during the reactor cycle.

full reactor cycle.

Neutron fluxes in the external moderator and experimental channels

Inside the external reflector tank of the reactor, neutrons are moderated by the heavy water, where the scattering length is about 20cm. The moderator partly reflects the thermalized neutrons towards the fuel element. It is evident that different neutron spectra will be present at different distances from the core (with an increase of the moderation as a function of the distance). Starting from about 60cm from the fuel element edge, the spectrum is essentially a Maxwellian distribution at the moderator temperature.

In Fig. 5 we present the neutron fluxes calculated at different distances from the central

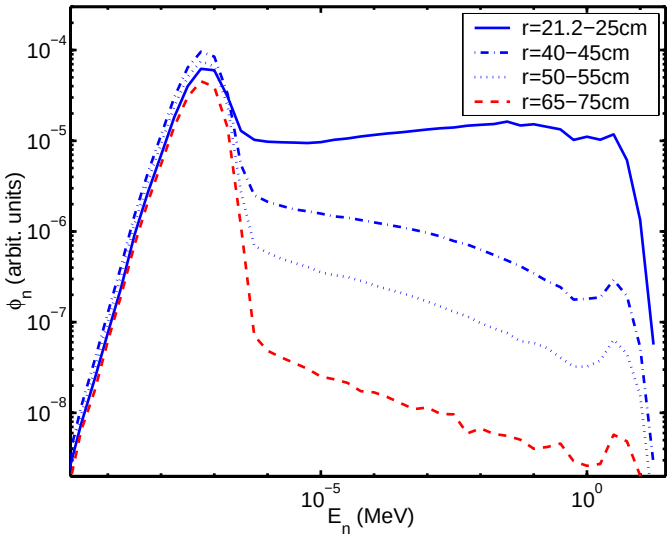

Figure 5: Neutron spectra in the external reflector for different radial distances r from the central axis of the core.

axis of the reactor core. Thermal neutrons become dominant (>90%) at about 40cm (dashed-dotted line). As close as at 5-10cm from the reactor core, nearly ∼56% of the neutrons are still epithermal and/or fast (solid line).

The schemes of the installation of an inclined V4 and horizontal H9 beam tubes are presented on the left and right part of Fig. 6 respectively. This particular geometry has been used for our simulations with the MCNP code.

The transmutation samples can be positioned at different distances along the experimental channels (V4 and H9) to have access to variable neutron fluxes. For comparison in Fig. 7 we show calculated neutron fluxes in the lowest/end positions of V4 and H9 beam tubes, where flux intensities of $1.78\times10^{15}\frac{n}{s\,cm^2}$ and $7.6\times10^{14}\frac{n}{s\,cm^2}$ respectively are predicted at nominal reactor power of $58\mathrm{MW}_{th}$. These values are the neutron fluxes averaged over entire fuel cycle (see Table 3).

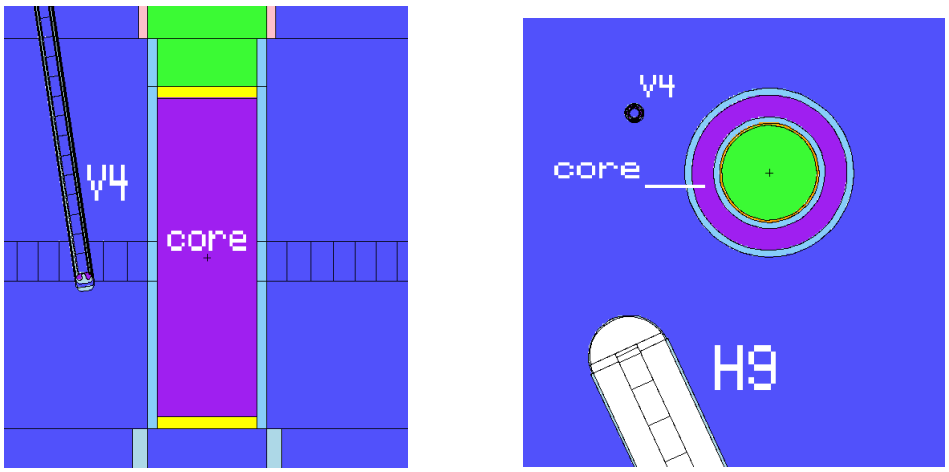

Figure 6: Positions of V4 (vertical) and H9 (horizontal) experimental tubes with respect to the fuel element (core).

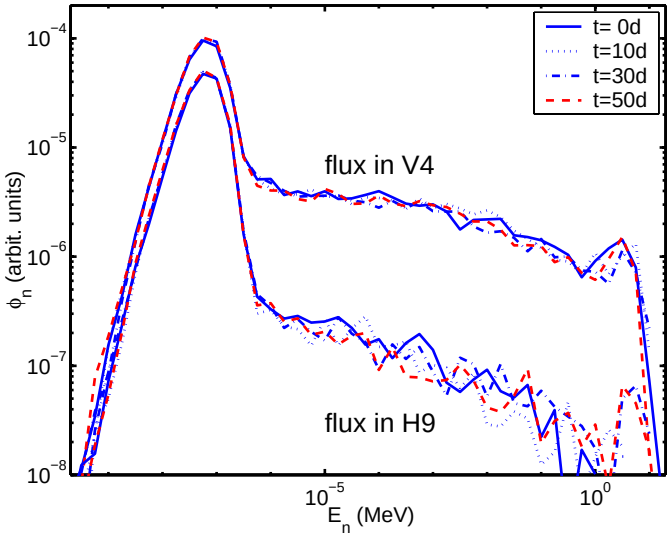

Figure 7: Calculated neutron fluxes at the lowest/end positions of the experimental beam channels V4 and H9 depending on time t (days) of the reactor cycle. Also see Fig. 6.

As long as the energy spectra of neutrons are concerned, we found that the flux in H9 is more thermalized (∼98.3%) if compared to the flux in V4 (∼85.2%). The calculated change (due to fuel burnup and move of the control rod) of the thermal part of the flux is not higher than 1% in both

channels. We remind that inside the fuel element at the end of the fuel cycle the contribution of the thermal neutrons was increased by ∼7% as shown in Fig. 4. However, in the external reflector (including experimental channels) most of the epithermal and fast neutrons leaving the reactor core become thermal, and this already small change of ∼7% becomes relatively less important further away from the reactor core.

We have to note at this point, that the fluxes calculated in H9 experimental channel are by ∼25% higher than the corresponding experimentally measured values, namely 5.5-5.9$\times 10^{14}\frac{n}{s\,cm^2}$ with 10% uncertainty [10]. We believe, that the major reason for overestimation of this flux in absolute value was due to many other experimental channels [2] which where not taken in account in our simulated geometry. Secondly, only after when all calculations had been finished, we have realized that the mass of U-235 in the initial fuel load (see Table 1) was not taken correctly, i.e. 8.0kg of U-235 instead of 8.6kg [2]. Finally, the calculated average neutron fluxes correspond to the H9 experimental channel filled with heavy water but not with air as it was the case during the experiment [10]. Therefore, we have performed a new calculation (at time t=0days), now with a correct mass of U-235 and no heavy water in the experimental tube H9. The calculated flux has decreased by 15%, i.e. from $7.9\times 10^{14}\frac{n}{s\,cm^2}$ down to $6.7\times 10^{14}\frac{n}{s\,cm^2}$, which is in a better agreement with the experimentally obtained value. Similar decrease was predicted for the flux in the experimental channel V4, namely from $1.88\times 10^{15}\frac{n}{s\,cm^2}$ down to $1.65\times 10^{15}\frac{n}{s\,cm^2}$.

Finally, we add that the above correction for the absolute value of the neutron fluxes does not change the conclusions we made concerning the energy spectra of neutrons during the fuel cycle. However, the fuel burnup would be slightly smaller than presently predicted value of ∼47%.

Conclusions

We have performed a quantitative calculations of the evolution of the fuel and fluxes of the figh flux reactor at ILL Grenoble for its full reactor cycle. The simulations were done with two different code systems: *Monteburns* (MCNP+ORIGEN2) and MCNP+CINDER'90. The major difference between two codes is that the first is based on one-group neutron cross section libraries while the second uses 63-group neutron data.

Both codes reproduce correctly the history of the fuel cycle (k_{eff} ∼1 at all times within 50 days) and give similar fuel burnup of ∼47%. Calculated average neutron flux (corrected as discussed above) in the reactor core is $2.16\times 10^{15}\frac{n}{s\,cm^2}$ and decreases down to $1.65\times 10^{15}\frac{n}{s\,cm^2}$ and $6.7\times 10^{14}\frac{n}{s\,cm^2}$ in the experimental channels V4 and H9 respectively at the lowest/end positions. Thermal neutron (E_n <1eV) contribution is ∼85.2% in V4 and ∼98.3% in H9.

In both experimental channels (V4 and H9) there were no important changes (within 1%) in the energy spectra of the neutrons due to fuel evolution and/or move of the control rod. On the other hand, the contribution of the thermal neutrons increased by 7% in the fuel element (core) itself at the end of the reactor cycle.

We conclude that neutron fluxes in the experimental channels V4 and H9 are not perturbed/changed due to the burnup of the fuel element and/or move of the control rod. We believe that this result simplifies most of the irradiation experiments (and data analysis in particular), which employ the experimental channels as above. The Mini-Inca project is one of them.

Finally, this work serves as a validation study of two different evolution codes, namely ORIGEN2 and CINDER'90. It also gives us confidence to employ them for the simulations of different critical or sub-critical systems related to nuclear waste transmutation. The calculations along these lines are in progress [11].

References

[1] G. Fioni *et al.*, "Mini-Inca: Integral Measurements Relevant for Nuclear Waste Transmutation Systems", Preposition au Conseil Scientifique et Technique, SPhN CEA/Saclay, France (December 1998).

[2] "Rapport De Surete Du Reacteur A Haut Flux", Vol. **4**, Institut Max von Laue - Paul Langevin, (Grenoble 1971).

[3] H.R. Trellue and D.I. Poston, "User's Manual, Version 2.0 for Monteburns, Version 5B", Los Alamos National Laboratory, *preprint* **LA-UR-99-4999** (1999); H.R. Trellue, private communication (April 2000).

[4] J. Briesmeister for Group X-6, "MCNP-A, A General Monte Carlo Code for Neutron and Photon Transport", Version 4A, Los Alamos National Laboratory, *preprint* **LA-12625-M** (1993).

[5] RSIC Computer Code Collection, "ORIGEN 2.1 - Isotope Generation and Depletion Code Matrix Exponential Method", Radiation Shielding Information Center, *report* **CCC-371** (1991).

[6] ENDF/B-VI, "The US evaluated neutron nuclear data library for neutron reactions", IAEA-Vienna, IAEA-NDS-100, Rev. **6** (1995).

[7] JENDL-3.2, "The Japanese Evaluated Nuclear Data Library", IAEA-Vienna, IAEA-NDS-110, Rev. **5** (1994).

[8] JEF-2.2, "The evaluated neutron nuclear data library of the NEA Data Bank", IAEA-Vienna, IAEA-NDS-120, Rev. **3** (1996).

[9] W.B. Wilson, T.R. England and K.A. Van Riper, "Status of CINDER'90 Codes and Data", Los Alamos National Laboratory, *preprint* **LA-UR-99-361** (1999), submitted to Proc. of 4th Workshop on Simulating Accelerator Radiation Environments, September 13-16, 1998, Knoxville, Tennessee, USA; W.B. Wilson, private communication (March 2000).

[10] F. Gunsing, G. Fioni, "Neutron flux determination from iron monitors for the ^{241}Am transmutation experiment", CEA-report, DAPNIA/SPhN **98-07** (1998).

[11] P. Goberis, "Modelling of innovative critical reactors with thermalized neutron fluxes in the frame of the Mini-Inca project", *rapport du stage* at DAPNIA/SPhN, CEA Saclay (2000).

time, days	k_{eff}	ϕ_n(core), $10^{15}\frac{n}{s\,cm^2}$	ϕ_n(V4), $10^{15}\frac{n}{s\,cm^2}$	ϕ_n(H9), $10^{15}\frac{n}{s\,cm^2}$	^{235}U (g)	^{238}U (g)	^{239}Pu (g)	^{135}Xe (g)	^{149}Sm (g)
0.0	1.039	2.25	1.88	0.79	7970	607	0.00	0.000	0.00
0.5	1.037	2.30	1.71	0.78	7930	607	0.01	0.045	0.01
1.0	1.035	2.27	1.71	0.72	7890	607	0.05	0.055	0.02
2.0	1.038	2.27	1.65	0.75	7820	606	0.27	0.060	0.08
5.0	1.037	2.28	2.00	0.74	7590	604	1.54	0.062	0.26
10.	1.034	2.30	1.88	0.75	7210	600	4.36	0.058	0.36
15.	1.031	2.30	1.75	0.75	6830	596	7.15	0.054	0.37
20.	1.041	2.31	1.74	0.74	6450	592	9.64	0.051	0.37
25.	1.042	2.32	1.70	0.76	6070	589	11.7	0.047	0.37
30.	1.047	2.32	1.71	0.77	5690	585	13.3	0.044	0.36
35.	1.047	2.36	1.78	0.74	5310	581	14.7	0.041	0.36
40.	1.048	2.39	1.66	0.72	4940	577	15.8	0.038	0.35
45.	1.042	2.43	1.98	0.79	4560	573	16.5	0.035	0.34
50.	1.041	2.46	1.83	0.77	4180	570	16.8	0.031	0.33
Average	1.040	2.32	1.78	0.76					

Table 3: Ractor full cycle history (*Monteburns* simulation). The eigenvalue problem for k_{eff} with MCNP has been run with 125,000 source neutrons.

time, days	k_{eff}	^{235}U (g)	^{238}U (g)	^{239}Pu (g)	^{135}Xe (g)	^{149}Sm (g)
0.0	1.037	7970	607	0.00	0.000	0.00
0.5	1.030	7929	607	0.00	0.049	0.01
1.0	1.027	7891	607	0.03	0.064	0.04
2.0	1.025	7818	607	0.09	0.069	0.11
5.0	1.024	7596	606	0.46	0.067	0.30
10.	1.023	7229	605	1.27	0.064	0.40
15.	1.031	6874	604	2.09	0.061	0.42
20.	1.016	6536	603	2.82	0.058	0.43
25.	—	6136	602	3.44	0.054	0.40
30.	1.022	5760	601	4.02	0.051	0.42
35.	—	5360	600	4.47	0.046	0.40
40.	1.023	4989	599	4.89	0.043	0.41
45.	—	4607	598	5.16	0.039	0.38
50.	1.008	4255	597	5.42	0.036	0.39
Average	1.024					

Table 4: Ractor full cycle history (MCNP+CINDER'90 simulation). The eigenvalue problem for k_{eff} with MCNP has been run with 2,000,000 source neutrons. Note: k_{eff} values and fluxes were not calculated at t=25, 35 and 45 days.